Engineering Science and Technology, an International Journal 18 (2015) 727–737

HOSTED BY

Contents lists available at ScienceDirect

Engineering Science and Technology, an International Journal

journal homepage: http://www.elsevier.com/locate/jestch

Full length article

Heat transfer optimization of two phase modeling of nanofluid in a sinusoidal wavy channel using Artificial Bee Colony technique

P. Valinataj-Bahnemiri [a], A. Ramiar [a,*], S.A. Manavi [a], A. Mozaffari [b]

[a] Faculty of Mechanical Engineering, Babol Noshirvani University of Technology, P.O. Box 484, Babol, Iran
[b] Department of Systems Design Engineering, University of Waterloo, Waterloo, ON, Canada N2L 3G1

ARTICLE INFO

Article history:
Received 13 March 2015
Received in revised form
9 May 2015
Accepted 10 May 2015
Available online 16 June 2015

Keywords:
Heat transfer optimization
Nanofluids
Mixture method
Artificial Bee Colony algorithm
Wavy channel

ABSTRACT

The present study represents the heat transfer optimization of two-dimensional incompressible laminar flow of Al_2O_3-water nanofluids in a duct with uniform temperature corrugated walls. A two phase model is applied to investigate different governing parameters, namely: Reynolds number ($100 \leq Re \leq 1000$), nonofluids volume fraction ($0\% \leq \phi \leq 5\%$) and amplitude of the wavy wall ($0 \leq \alpha \leq 0.04$ m). For optimization process, a recent spot-lighted method, called Artificial Bee Colony (ABC) algorithm, is applied, and the results are shown to be in a good accuracy in comparison with another well-known heuristic method, i.e. particle swarm optimization (PSO). The results indicate that the effect of utilizing nanoparticles and increasing Reynolds number is more intensified on growing the average Nusselt number than variations of the amplitude of the wavy wall. To prevent the worst possible heat transfer, the specific amplitude which leads to a minimum average Nusselt number is detected. The effect of using nanoparticles on thermal-hydraulic performance factor (j/f) is presented which considers both heat transfer and hydrodynamics aspects. The results showed that volume fraction has a direct and the wavy wall's amplitude has a converse effect on the thermal-hydraulic performance factor. Furthermore, an optimum value for Reynolds number is found to maximize the thermal-hydraulic performance factor.

1. Introduction

Optimization of heat transfer systems is of significant importance in many engineering applications, particularly those employing compact heat exchangers. Heat transfer enhancement methods can be divided into two categories. Active methods such as surface vibration, electrostatic fields, injection and suction, and passive methods such as extended surfaces, inserts, surface treatments and additives. Using wavy channels, as a passive method is a cheap and appropriate way for increasing the heat transfer in compact heat exchangers. As a matter of fact, wavy channels prevent the development of flow by disturbing the flow field and boundary layer, and improve the mixing of higher and lower temperature parts which enhance the heat transfer. Furthermore, increasing the thermal properties of fluid with suspending solid particles, in nano scale, is an innovative way to enhance the rate of heat transfer as a passive method, because of their higher thermal conductivities in comparison with common fluids. Various approximations can be used to simplify the computational task. The simplest approach is to represent the suspension by a homogeneous single-phase system and take into account the influence of particles by only changing the values of physical properties. In many practical applications of multiphase flow, the mixture model is sufficiently accurate. The mixture equations largely resemble those for a single-phase flow, but are represented in terms of the mixture, density and velocity. However, a supplementary term in the mixture momentum equation arises from the slip of the dispersed phases relative to the continuous phase.

Many researchers have studied the effects of the wavy wall on the heat transfer of conventional fluid. Wang and Chen [1] studied the rate of heat transfer in a sinusoidal wavy channel in the laminar regime with uniform wall temperature. They found that by increasing the Reynolds number and Prandtl number, the rate of both heat transfer and skin-friction increases, and there is not a significant enhancement in heat transfer at smaller amplitude wavelengths.

Mohamed et al. [2] numerically studied laminar forced convection at the entrance region of a wavy wall channel with constant

* Corresponding author.
E-mail address: aramiar@nit.ac.ir (A. Ramiar).
Peer review under responsibility of Karabuk University.

http://dx.doi.org/10.1016/j.jestch.2015.05.005

Nomenclature

C_p	constant pressure specific heat, J/kg K
f	friction factor
H	channel height, m
j	Colburn factor
K	thermal conductivity, W/m K
n	direction normal on walls
Nu	Nusselt number
ΔP	pressure drop, Pa
Pr	Prandtl number
Re	Reynolds number
T	temperature, K
U	velocity, m/s
x, y	spatial coordinates, m

Greek symbols

ϕ	volume fraction of nanoparticles
μ	dynamic viscosity, Pa s
ρ	density, kg/m^3
τ	wall shear stress, Pa
α	amplitude of wavy wall, m
λ	wavelength of wavy wall, m

Subscripts

ave	average
f	fluid properties
c	continuous phase
w	wall
k	k-th phase
m	mixture
nf	nanofluid properties
p	nanoparticles

wall heat flux. The Reynolds number was confined within the range of 100–1500, and the amplitude of the surface was between 0 and 0.5. Their results showed that the shear stress and the Nusselt number increase by increasing the Reynolds number and highest magnitude occurs in the entrance area.

Castellões et al. [3] reported convective heat transfer enhancement in low Reynolds number flows with wavy walls. They proposed a hybrid numerical-analytical solution methodology for energy equation. They achieved an illustrative sinusoidal corrugation shape, and discussed on the influence of Reynolds number and corrugation geometric parameters.

Metwally et al. [4] studied enhanced heat transfer due to curvature-induced lateral vortices in laminar flow in sinusoidal channels. They represented that increasing the Reynolds number results in the increasing of both Nusselt number and skin friction. Also, they found that in the non-circulating regime, the geometry of the channel didn't have a significant effect on the heat transfer enhancement. But in the circulating regime, flow separation and reattachment grow with Reynolds number and aspect ratio.

Some researchers applied the single-phase or two-phase model approach for the simulation of nanofluids. Manavi et al. [5] investigated the turbulent forced convection of Al_2O_3-water nanofluid in a wavy channel using two phase mixture model. The conducted simulations revealed that by increasing the volume fraction of nanoparticles, Reynolds number and amplitude of wall waves, the rate of heat transfer is increased. Moreover, the results indicated that the mixture model yields higher Nusselt numbers as compared to the single phase model.

Heidary and Kermani [6] investigated the effect of nanoparticles on laminar forced convection in sinusoidal-wall channel. For simulation of nanofluids, they used single phase model and found that adding nano-particles to pure fluid makes significant increase in heat transfer. They used copper-water nanofluids with volume fraction between 0 and 20% and Reynolds number in the range of 5–1500.

Ahmed et al. [7] numerically investigated the heat transfer enhancement in a wavy channel using nanofluid. They employed single phase approach and their governing parameters were Reynolds number and volume fraction in the range of 100–800 and 0–5%, respectively. It was observed that the enhancement of heat transfer mainly depends on the nanoparticles volume fraction, the amplitude of the wavy wall, and Reynolds number rather than the wavelength.

Akbari et al. [8] compared single phase and three different two-phase models to the model of laminar mixed convection of Al_2O_3-water in a horizontal tube. They found that the predictions obtained from the two-phase models were basically the same and two-phase models yielded closer predictions of the convective heat transfer coefficient to the experimental data than the single-phase model.

Many studies have investigated the heat transfer optimization of different thermal applications [9–16]. But, a few of them worked on the heat transfer optimization of the corrugated channels. The heat transfer optimization in a channel composed of a smooth and a corrugated wall under laminar flow conditions has been studied by Fabbri [17]. The numerical model is utilized in genetic algorithm (GA) to maximize the heat transfer by optimizing the corrugation profile. Some optimum corrugation profiles were presented.

Yang et al. [18] performed an optimization to design two-dimensional channel with heated wavy walls with nanofluid. The effects of governing parameters on heat transfer enhancement such as the Reynolds number ($250 \leq Re \leq 1000$), the particle volume concentration ($0\% \leq \phi \leq 5\%$), the wavy channel amplitude ($0 \leq \alpha \leq 0.3$) and the wavy numbers ($3 \leq \beta \leq 12$) on the enhancement of the nanofluid heat transfer have been investigated. They obtained a solution to optimize the thermal performance of the wavy channel.

In recent years, a new optimization technique called Artificial Bee Colony (ABC) algorithm becomes more and more popular after its development by Karaboga [19,20] in 2005, because of its capability for handling practical engineering problems. ABC is a fast convergent and easy handling algorithm, which has less control parameters than most of the other existing meta-heuristic techniques. This algorithm is applied to a wide spectrum of applications such as neural networks design, industrial engineering, electrical engineering, civil engineering and many others, as well as mechanical engineering and fluid mechanics. For instance, Sahin et al. [21] developed a new shell and tube heat exchanger optimization design approach by applying Artificial Bee Colony (ABC) algorithm to minimize the total cost of the equipments.

In the present study, the application of ABC algorithm is investigated in order to maximize the thermal and hydraulic performance of the forced convection of nanofluid in a wavy channel with a uniform wall temperature. The novelty of this study with respect to the field of utilizing wavy channels can be viewed from the utilization of an efficient optimization process, considering

two phase mixture model to account for slip velocity between phases, and optimizing thermal-hydraulic aspect of the uniform temperature wavy wall, which has been less considered in the literature. Important parameters such as nanoparticles volume fraction, the amplitude of the wavy channel and Reynolds number are considered as optimization variables. Furthermore, the results are compared to another well-known population-based optimization method, called particle swarm optimization (PSO) [22].

2. Overview of Artificial Bee Colony algorithm

ABC is an evolutionary algorithm simulated by the intelligent foraging behavior of honey bee swarm, developed by Karaboga [19,20] in 2005. The artificial bees are classified into three cooperative categories: employed, onlookers and scouts. In ABC, foraging bees search around the hive to measure the nectar amount of the food sources, which dedicates the value of the food sources. Every food source can be a possible solution of the problem, therefore, employed bees and onlookers cooperate to exploit the solutions and scout bees are to explore them. These operations take action in three distinct phases after initialization.

2.1. Control parameters and initial population

ABC employs three important control parameters: maximum cycle number (MCN) which is considered as the limitation condition, total number of food sources (SN) which is equal to the number of employed or onlooker bees, the number of cycles which a food source is assumed to be abandoned because it cannot be improved, which is named limit for abandonment (limit). The parameter values used in this study are as follows:

- Maximum cycle number (MCN): 40
- Number of food sources (SN) or employed bees (n_e) or onlooker bees (n_o): 5
- Colony size $= n_e + n_o$: 10
- Number of scout bees (n_s): 1
- Limit for abandonment (*limit*): 5

In the initialization of the algorithm, the food sources should be generated randomly by the following expression:

$$x_i^j = x_{\min}^j + \mathrm{rand}(0,1)\cdot\left(x_{\max}^j - x_{\min}^j\right) \quad i = 1,2,\ldots,\mathrm{SN} \quad j = 1,2,\ldots,D \tag{1}$$

where x_i^j represents the ith food source with the jth parameter. rand(0,1) is a real random number between [0,1]. D is the number of the optimization parameters. $x_{\min}^j$ and $x_{\max}^j$ are the lower and the upper bounds of the solution. After initialization, population is evaluated and subjected to repeat the foraging processes of the employed, onlooker and scout bees until the termination criteria are achieved.

2.2. The employed bee phase

In this phase, each employed bee modifies the old food source position as x_i^j to the new one in its neighborhood as v_i^j, and then, evaluates its quality. Position modification is calculated using the following expression:

$$v_i^j = x_i^j + \mathrm{rand}(-1,1)\cdot\left(x_i^j - x_k^j\right) \tag{2}$$

where k and j are randomly chosen indexes within the range of [1,SN] and [1,D], respectively. k must be different from i. rand(−1,1) is a real random number between [−1,1]. After evaluating the new food source positions, their fitness values must be calculated. In ABC, the fitness value is proportional to the nectar amounts of the food sources and shows how valuable a food source is. After that, a greedy selection mechanism is applied to memorize whether the current position of the food source is better or the previous one. The fitness value (fit_i) of each position i is calculated by the following expression, where f_i denotes the objective value of the ith solution:

$$\mathrm{fit}_i = \begin{cases} 1/(1+f_i), & \text{if } f_i \geq 0 \\ 1+|f_i|, & \text{if } f_i < 0 \end{cases} \tag{3}$$

2.3. The onlooker bee phase

At this step, employed bees share their knowledge of the food sources they have evaluated so far with onlooker bees in the hive, and then, onlookers search the nearby approved food sources using Eq. (2). Each onlooker bee does such exploitation by roulette wheel selection according to each food source's probability value (p_i) associated with it:

$$p_i = \frac{\mathrm{fit}_i}{\sum_{i=1}^{\mathrm{SN}} \mathrm{fit}_i} \tag{4}$$

2.4. The scout bee phase

After the exploitation job of employed and onlooker bees, they might be tired of some food sources they met so far, i.e. the food source is no longer of interest to be exploited. After some limited amount of trials, which is called limit for abandonment (limit), the food source will be deserted to cherish the chances of exploring better solutions. This exploration process is done by scout bees through Eq. (1), who are the employed bees retired from their duty.

In every cycle during the optimization process, the best solution so far is memorized, and this process goes on until the maximum cycle number (MCN) is reached.

3. Physical model and mathematical formulation

The 2D incompressible laminar flow in a wavy channel with constant wall temperature is analyzed. At the inlet, uniform velocity and temperature are assumed and there is no slip on surfaces; both wavy surfaces at the top and bottom are held at constant temperature ($T_w = 350$ K), and there is no slip on surfaces. At the outlet section of the duct, fully developed flow is considered. The geometry of the problem and employed mesh and other boundary conditions are shown in Fig. 1. There are six waves along the wavy wall and the wavelength of the wavy channel is considered to be constant and equal to 0.2 m. The working nanofluid is assumed to be Newtonian, the nanofluids temperature at the inlet is 300 K and the slip velocity between particles and the fluid is considered. The flow in the channel is assumed symmetric and only the bottom half of the channel is considered in this study.

The continuity and momentum equations of mixture model are as follows [23]:

Continuity equation for the mixture:

$$\frac{\partial \rho_m}{\partial t} + \nabla\cdot(\rho_m U_m) = 0 \tag{5}$$

where:

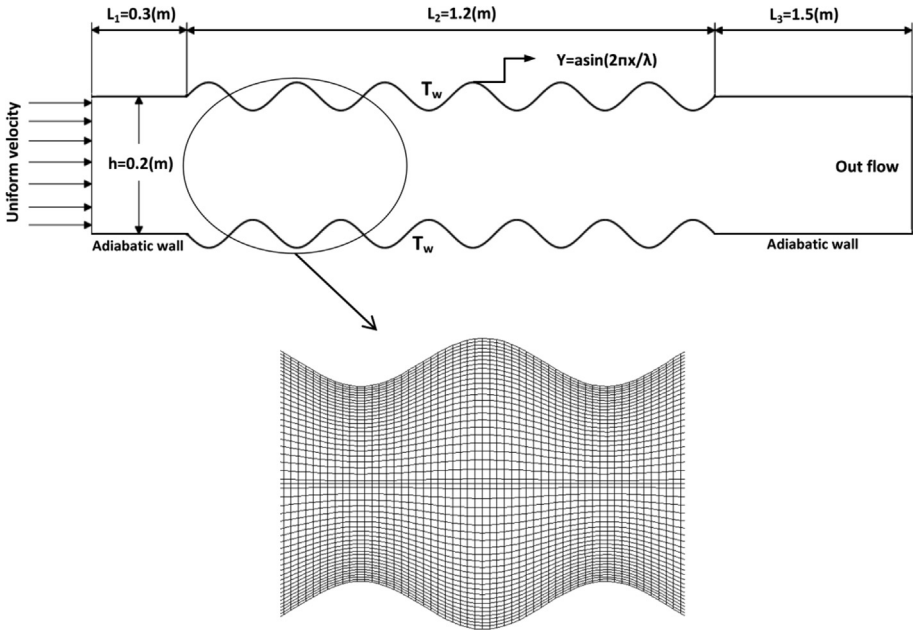

Fig. 1. Geometry of the problem and employed mesh for the geometry.

$$U_{\mathrm{m}} = \frac{1}{\rho_{\mathrm{m}}} \sum_{k=1}^{n} \phi_k \rho_k u_k = \sum_{k=1}^{n} c_k u_k \tag{6}$$

Continuity equation for the dispersed phase (nanoparticles):

$$\frac{\partial \phi_{\mathrm{p}}}{\partial t} + \nabla \cdot (\phi_{\mathrm{p}} U_{\mathrm{m}}) = -\nabla \cdot \left[\phi_{\mathrm{p}} \phi_{\mathrm{c}} \frac{\rho}{\rho_{\mathrm{m}}} (U_{\mathrm{p}} - U_{\mathrm{c}}) \right] \tag{7}$$

Momentum equation for the mixture:

$$\begin{aligned} \frac{\partial \rho_{\mathrm{m}} U_{\mathrm{m}}}{\partial t} + \nabla \cdot (\rho_{\mathrm{m}} U_{\mathrm{m}} U_{\mathrm{m}}) = -\nabla p + \nabla \cdot \tau_{\mathrm{Gs}} + \rho_{\mathrm{m}} g \\ -\nabla \cdot \left[\phi_{\mathrm{p}} \rho_{\mathrm{p}} \left(1 - \frac{\phi_{\mathrm{p}} \rho_{\mathrm{p}}}{\rho_{\mathrm{m}}} \right) \right. \\ \left. \times (U_{\mathrm{p}} - U_{\mathrm{c}})(U_{\mathrm{p}} - U_{\mathrm{c}}) \right] \end{aligned} \tag{8}$$

$$\tau_{\mathrm{Gs}} = (\mu_{\mathrm{m}}) \left[\nabla U_{\mathrm{m}} + (\nabla U_{\mathrm{m}})^T \right]$$

Momentum equation for the dispersed phase (slip velocity equation):

$$|U_{\mathrm{p}} - U_{\mathrm{c}}|(U_{\mathrm{p}} - U_{\mathrm{c}}) = \frac{4 d_{\mathrm{p}}}{3 C_{\mathrm{D}}} + \left(\frac{\rho_{\mathrm{p}} - \rho_{\mathrm{m}}}{\rho} \right) \left[g - (U_{\mathrm{m}} \cdot \nabla) U_{\mathrm{m}} - \frac{\partial U_{\mathrm{m}}}{\partial t} \right] \tag{9}$$

where:

$$\begin{cases} C_{\mathrm{D}} = \begin{cases} 24(1 + 0.1 Re_{\mathrm{p}} \le 1000) \\ 0.45 \left(\dfrac{1 + 17.67 f(\phi_{\mathrm{p}})^{\frac{6}{7}}}{18.87 f(\phi_{\mathrm{p}})} \right), \quad Re_{\mathrm{p}} > 1000, \\ f(\phi_{\mathrm{p}}) = \sqrt{1 - \phi_{\mathrm{p}}} \left(\dfrac{\mu_{\mathrm{c}}}{\mu_{\mathrm{m}}} \right) \end{cases} \\ Re_{\mathrm{p}} = \left(\dfrac{dp \sqrt{u_{\mathrm{cp}_0}^2 + v_{\mathrm{cp}_0}^2} \rho_{\mathrm{f}}}{\mu_{\mathrm{m}}} \right), \\ \begin{cases} \mu_{\mathrm{m}} = \mu_{\mathrm{f}} \left(1 - \dfrac{\alpha_{\mathrm{p}}}{\alpha_{\mathrm{pm}}} \right)^{-2.5 \alpha_{\mathrm{pm}} \mu^*} \\ \mu^* = 1, \ \alpha_{\mathrm{pm}} = 0.62 \end{cases} \end{cases} \tag{10}$$

The energy equation for the 2D flow problem is given by Ishii et al. [24]:

$$\begin{aligned} \nabla \cdot (\rho_{\mathrm{m}} U_{\mathrm{m}} C p_{\mathrm{m}} T) = \nabla \cdot (K_{\mathrm{m}} \nabla T_{\mathrm{m}}) - \\ \nabla \cdot \left(\phi_{\mathrm{p}} \frac{\rho_{\mathrm{f}} \rho_{\mathrm{p}}}{\rho_{\mathrm{m}}} U_{2j} T \left((c_{\mathrm{p}})_{\mathrm{f}} - (c_{\mathrm{p}})_{\mathrm{p}} \right) \right) \end{aligned} \tag{11}$$

where U_{2j} is drift velocity defined as:

$$U_{2j} = -\phi_{\mathrm{p}} (U_{\mathrm{c}} - U_{\mathrm{p}}) \tag{12}$$

The non-dimensional flow and heat transfer parameters are defined as [24]:

$$Re = \frac{2 \rho_{\mathrm{nf}} U_{\mathrm{in}} h}{\mu_{\mathrm{nf}}} \tag{13}$$

$$Nu = \frac{2 h k_{\mathrm{m}} \partial T / \partial n}{\left(k_{\mathrm{f}} (T_{\mathrm{w}} - T_{\mathrm{in}}) \right)} \tag{14}$$

The average Nusselt number is obtained by integrating the local Nusselt number along the bottom surface as follows:

$$Nu_{ave} = \frac{\int Nu \cdot ds}{S} \tag{15}$$

3.1. Thermal properties of nanofluid

3.1.1. Effective thermal conductivity

The thermal conductivity of the nanofluid is calculated from the following equation introduced by Ishii et al. [24]:

$$K_m = (1 - \phi_p) \times K_f + \phi_p \times K_p \tag{16}$$

3.1.2. Density and specific heat

The density and specific heat of the nanofluids are measured by applying the Pak and Cho [25] correlations, which are defined as follows:

$$\begin{aligned} \rho_m &= \sum_{k=1}^{n} \phi_k \rho_k \\ (c_p)_m &= \frac{\left((1 - \phi_p) \times \rho_f \times (c_p)_f + \phi_p \times (\rho \times c_p)_p\right)}{\rho_m} \end{aligned} \tag{17}$$

Thermal heat transfer is characterized by the j Colburn factor which is calculated from [26]:

$$j = \frac{Nu \times Pr^{-\frac{1}{3}}}{Re} \tag{18}$$

And pressure drop of wavy channel can be expressed in terms of friction factor [26]:

$$f = \left(\frac{2\Delta P}{\rho U_{ave}^2}\right)\left(\frac{2h}{L_2}\right) \tag{19}$$

The improvement of heat transfer performance of swirling flow in corrugated channels is also accompanied with an increase in the pressure drop. Consequently, it is important to evaluate the applicability of using nanofluids in channels. One method of estimating the relative thermal-hydraulic performance enhancement is to consider j/f ratio defined as [26]:

$$j/f = \frac{Nu \times \mathrm{Pr}^{-\frac{1}{3}}}{\mathrm{Re} \times f} \tag{20}$$

4. Numerical procedure and validations

In this paper, finite volume approach on a collocated grid is applied to discretize the governing equations inside the computational domain. The momentum interpolation approach of Rhie and Chow is employed in SIMPLE algorithm to link the pressure and velocity fields (Ferziger and Peric [27]). For the stability of the solution, the diffusion term in the momentum equations is approximated by the second order central difference. Moreover, a deferred correction scheme is adopted for the convective terms. The results have been obtained for grid densities of 200 × 20, 300 × 25, 400 × 30 and 500 × 30, in the corrugated section, for the sake of mesh independency. According to the results as shown in Fig. 2, the 400 × 30 density has a good accuracy and optimum run time figure. As investigated by Manavi et al. [5], the mixture model yields higher Nusselt numbers, and predicts the treatment of the two phase mixture more precisely. Hence, this method is applied for the results shown in the rest of the paper. For more detailed information, flowchart of the developed code, coupling ABC optimization code with the CFD code is illustrated in Fig. 3.

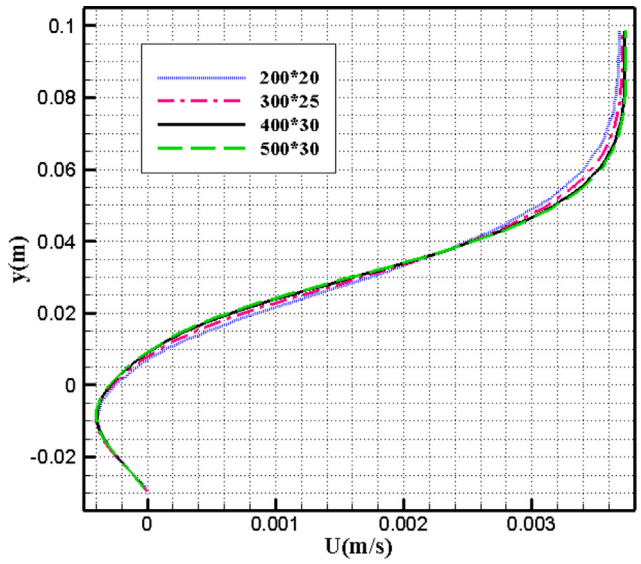

Fig. 2. Symmetric velocity profile at $x = 0.55$ m for mesh independency investigation when $Re = 1000$, $\alpha = 0.03$ m and $\phi = 2\%$.

For validation, the present study has been compared to the empirical and numerical investigations. The experimental study of Tolentino et al. [28] for $Re = 470$ and numerical results performed by, Yang et al. [18] for $Re = 500$, $\alpha = 0.02$ m and $\phi = 0\%$ were used for this purpose. The present results are in good agreement with the above mentioned numerical and experimental data as plotted in Fig. 4.

5. Optimal process

In present study, the maximum values of thermal-hydraulic performance factor (j/f) are achieved through optimized parameter values of Reynolds number, to improve the heat transfer performance accompanied by diminished pressure drop. In addition, the minimum values of Nusselt number are found through optimized parameter values of amplitude of the wavy wall, to detect the critical amplitudes and the worst circumstances which should be prevented in designing procedure. For optimization process, a very recent method named Artificial Bee Colony (ABC) algorithm was applied in this study. Also, a very well-known method named particle swarm optimization (PSO) is employed to validate ABC's results. It is worth mentioning that several runs for each case were assigned to ensure the accuracy of the results.

6. Results and discussion

Fig. 5 demonstrates the effects of wavy wall amplitude and Reynolds number on the average Nusselt number of the wavy wall. By increasing the Reynolds number, average Nusselt number increases. It can be noted that high velocity of the flow in the converging section of the wavy wall increases the heat transfer. Although, because of the swirl zones in diverging area, heat transfer decreases, but the average Nusselt number is more influenced by the high velocity flow of higher Reynolds numbers. Another

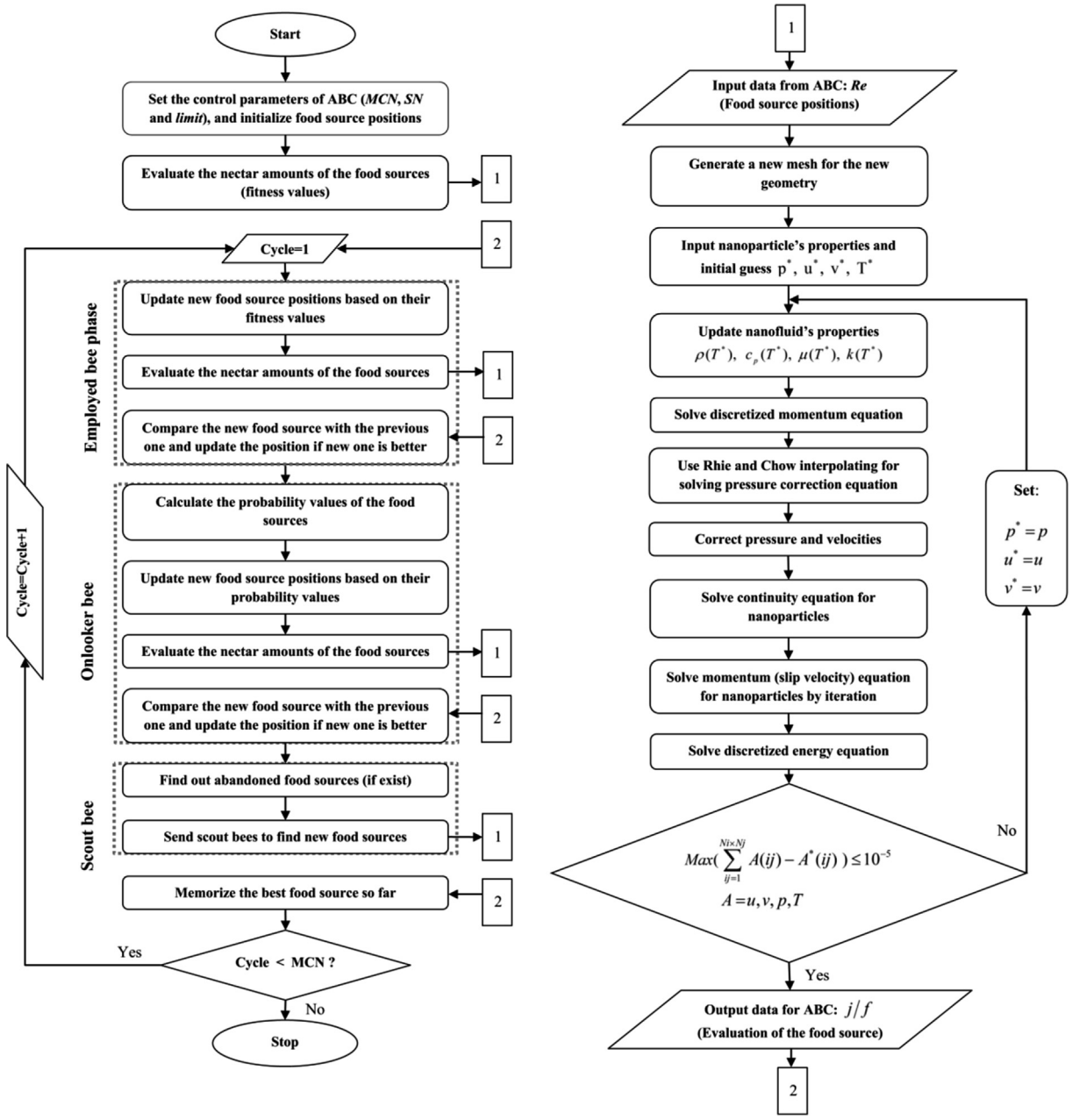

Fig. 3. Flowchart of the developed code.

observation is that for each Reynolds number, there is an amplitude which leads to the minimum average Nusselt number. It shows that increasing the amplitude leads to a decrement in average Nusselt number, but after a specific amplitude, Nusselt number increases. This behavior is due to the variation of heat transfer coefficient, which is proportional to the velocity of the flow. The velocity distribution for $Re = 500$ and $\phi = 2\%$ is represented in Fig. 6. $\alpha = 0.0216$ m is the amplitude found by optimization process, which will be presented among other results in later sections, leading to the minimum average Nusselt number for $Re = 500$ and $\phi = 2\%$. It can be found that by increasing the amplitude, velocity increases at the middle part of the channel, and decreases at other regions. By growing the amplitude until $\alpha = 0.0216$ m, the amount of decrement in the velocity is more than the amount of increment; which results in a lower heat transfer coefficient, and consequently less Nusselt number. But, for the amplitudes higher than $\alpha = 0.0216$ m, the rate of increment in velocity is more than its decrement, which leads to a higher heat transfer coefficient, and also higher Nusselt number. It should be noted that the variations of average Nusselt number versus amplitude of the wavy channel are not similar to those presented by Wang and Chen [1], which is due to their different definition of average Nusselt number.

The effect of volume fraction at different amplitudes on average Nusselt number is shown in Fig. 7. It is observed that when nanoparticles volume fraction increases, the average Nusselt number increases. When ϕ increases, inertia forces increase, causing the temperature gradient to be enhanced. Besides, the thermal conductivity ratio term in Eq. (14) increases too. Therefore, an increment in both volume fraction and thermal conductivity ratio leads to a higher average Nusselt number. In addition, like Fig. 5, for

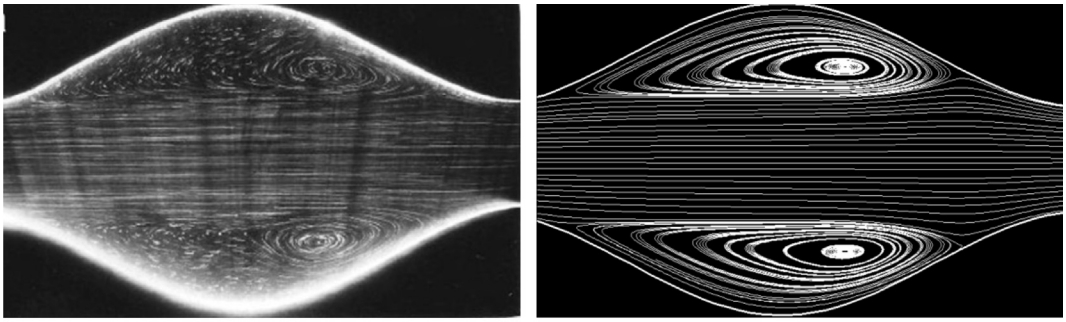

(a)

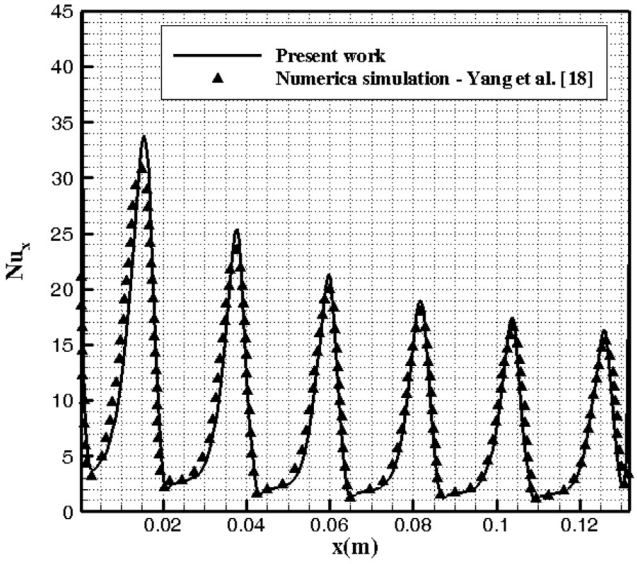

(b)

Fig. 4. (a) Stream lines validation with experimental results of Tolentino et al. [28] at $Re = 470$. (b) Local Nusselt number at $Re = 500$, $\alpha = 0.02$ m and $\phi = 0\%$.

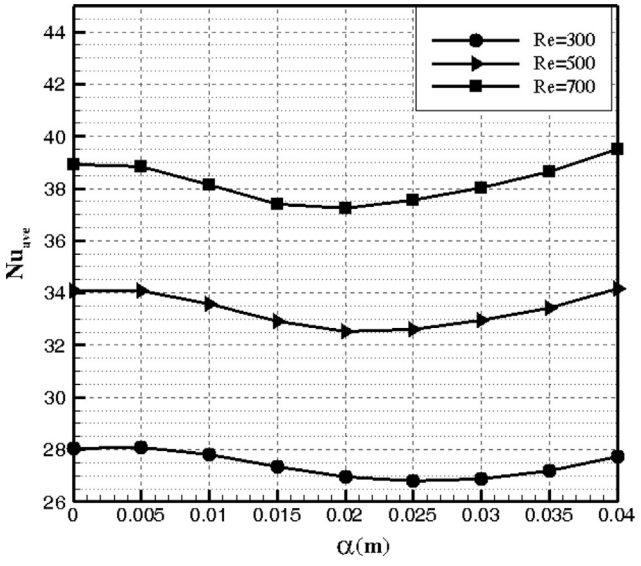

Fig. 5. Effects of amplitude and Reynolds number on average Nusselt number at $\phi = 2\%$.

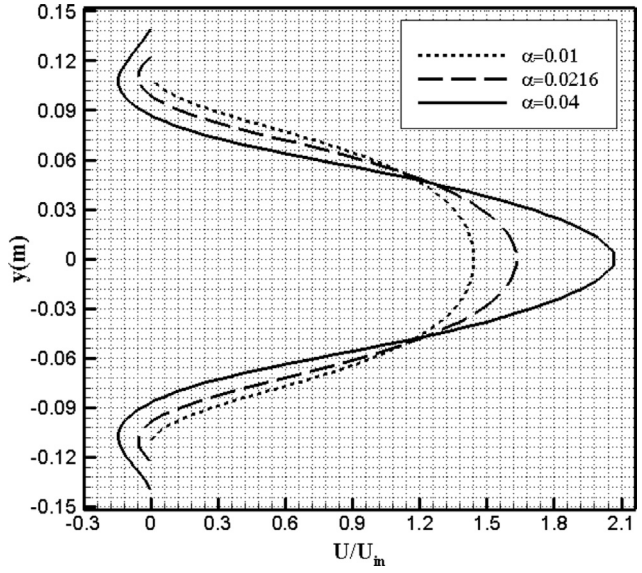

Fig. 6. Velocity distribution of various amplitudes at $x = 0.95$ m, $Re = 500$ and $\phi = 2\%$.

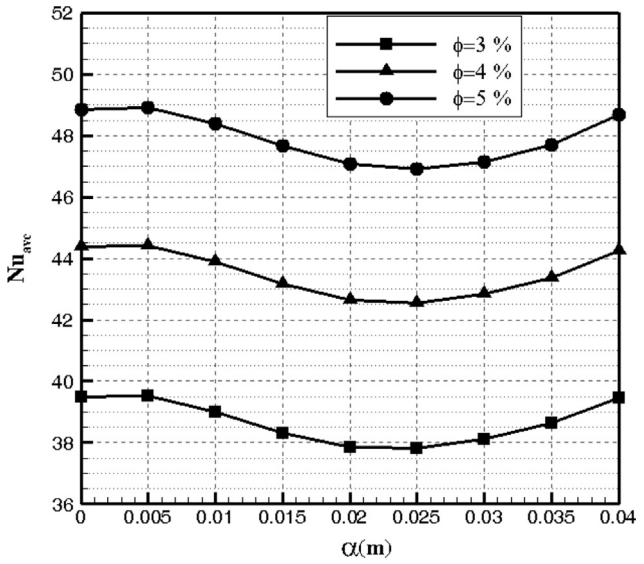

Fig. 7. Effect of volume fraction at different amplitudes on average Nusselt number when $Re = 500$.

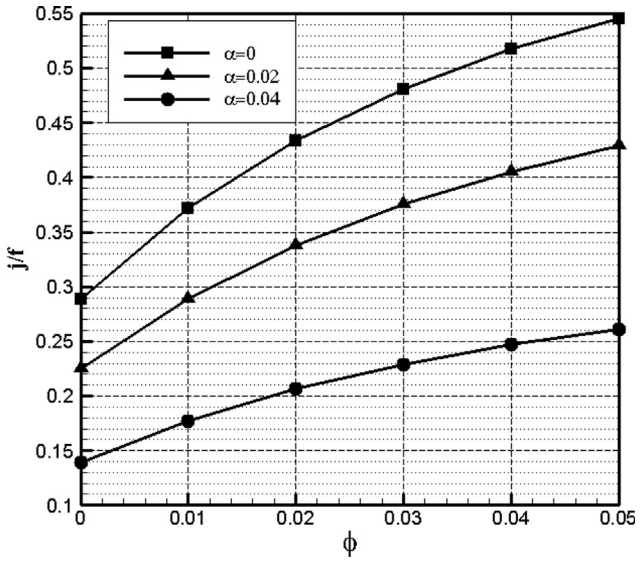

Fig. 9. Effect of amplitude size of the wavy wall at different volume fractions on (j/f) ratio at $Re = 700$.

each nanoparticles volume fraction, there is an amplitude which leads to the minimum average Nusselt number.

Fig. 8 illustrates the effects of Reynolds number and volume fraction on thermal-hydraulic performance factor (j/f). With increasing Reynolds number, j/f ratio increases until a maximum value, and then gradually declines. This shows that for each volume fraction, there is a Reynolds number which leads to the maximum thermal-hydraulic performance factor. As *Re* increases, both average Nusselt number and pressure drop increase. On the other hand, in lower *Re* numbers the growth rate of the average Nusselt number with *Re* is high and then decreases. In contrast, the growth rate of the pressure drop with *Re* is low at first and then increases, which justifies the behavior of j/f ratio. This shows that for each volume fraction, there is a Reynolds number which leads to the maximum thermal-hydraulic performance factor. j/f parameter considers the simultaneous effect of Nusselt number and pressure drop (f). It increases with increasing the Nusselt number and decreasing pressure drop. Although Reynolds number and volume fraction increase the Nusselt number (causing j/f to increase), but they raise the pressure drop too (leading j/f to decrease), and so they may increase or decrease j/f based on the prominence of Nusselt number or pressure drop. According to Fig. 8 in a constant volume fraction, increasing Reynolds number causes the j/f to increase for lower Reynolds numbers (raising pressure drop dominates) and decrease for higher Reynolds numbers (decrementing Nusselt number dominates).

Moreover, Fig. 8 indicates that by increasing of volume fraction, the j/f ratio increases. By increasing nanoparticles volume fraction, there is an increment in average Nusselt number as well as pressure drop. However, the increment in Nusselt number is much higher than the increment in pressure drop, which leads to an increment in j/f ratio.

The effect of amplitude of the wavy wall at different volume fractions on j/f ratio is depicted in Fig. 9. As seen, j/f ratio reduces with amplitude. By increasing the amplitude, pressure drop is augmented, because of the disturbance of the entire flow field. As mentioned before in Fig. 5, the behavior of average Nusselt number for different amplitudes is sinusoidal, but its order is remarkably

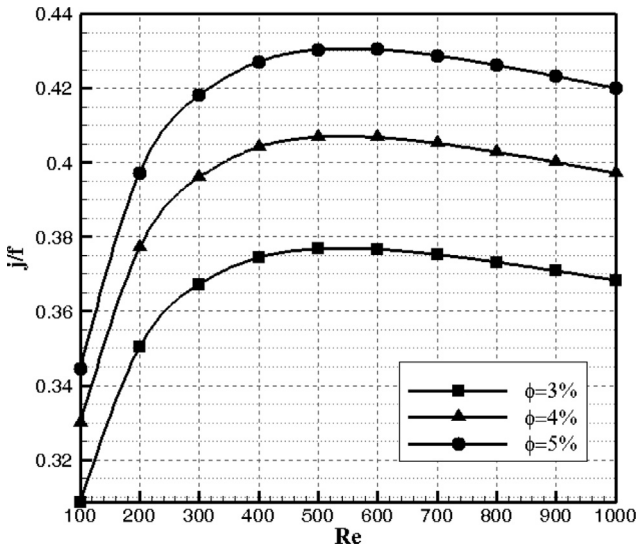

Fig. 8. Effects of Reynolds number and volume fraction on j/f ratio at $\alpha = 0.02$ m.

Table 1
Optimized values of Reynolds number and related maximum thermal-hydraulic performance factor with different volume fractions for two cases of $\alpha = 0.02$ m and $\alpha = 0.04$ m.

$\alpha(m)$	ϕ (%)	Optimized *Re*	j/f_{max}
0.02	0	671	0.225924
0.02	1	582	0.2909527
0.02	2	548	0.3405875
0.02	3	543	0.3792856
0.02	4	545	0.409641
0.02	5	552	0.4333917
0.04	0	342	0.1480496
0.04	1	324	0.1900699
0.04	2	319	0.2218382
0.04	3	318	0.2464522
0.04	4	320	0.2656948
0.04	5	323	0.2807239

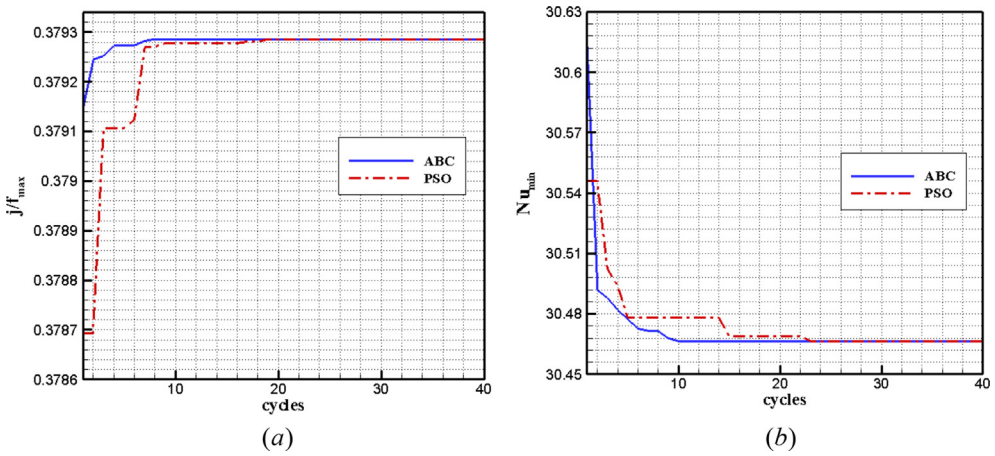

Fig. 10. Fitness values of, (a) maximum thermal-hydraulic performance factor for the case of $\alpha = 0.02$ m and $\phi = 3\%$, and, (b) minimum average Nusselt number for the case of $Re = 700$ and $\phi = 1\%$, versus cycle numbers.

less than the order of increment in pressure drop, which leads to a lower j/f ratio.

The plots in Fig. 10 show the variation of fitness values through cycle numbers for (a) maximum thermal-hydraulic performance factor in $\alpha = 0.02$ m and $\phi = 3\%$, and (b) minimum average Nusselt number for $Re = 700$ and $\phi = 1\%$. The plots indicate that the results of the two algorithms are in a good agreement, and for both optimization algorithms, we will gain the same results after several limited cycle numbers, but the convergence speed of ABC algorithm is comparatively higher than PSO procedure.

The detected Reynolds numbers by optimization algorithms which lead to the maximum thermal-hydraulic performance factor (j/f) as the objective function, for various volume fractions and wavy amplitudes are listed in Table 1. For example, for the case of $\alpha = 0.02$ m and $\phi = 2\%$ the thermal-hydraulic performance factor is enhanced up to 22.03%. For comparison purposes, for the case of $\alpha = 0.02$ m and $\phi = 2\%$, streamline and temperature contours of the optimized Reynolds number ($Re = 548$), and two other Reynolds numbers are displayed in Fig. 11. It is found that, by raising Reynolds number, flow near the wavy section becomes more disturbed, and

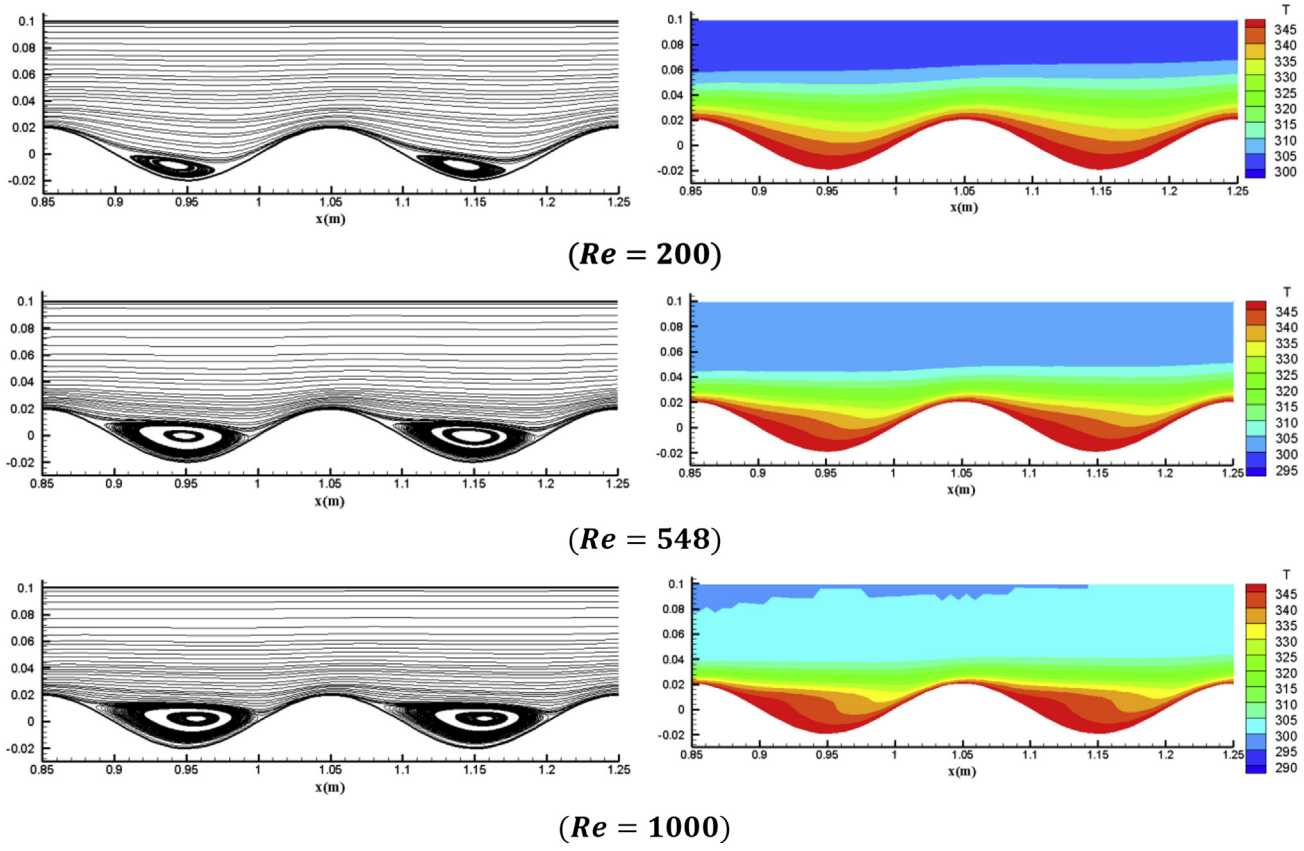

Fig. 11. Comparison of the streamline and temperature contours for different Reynolds numbers at $\alpha = 0.02$ m and $\phi = 2\%$.

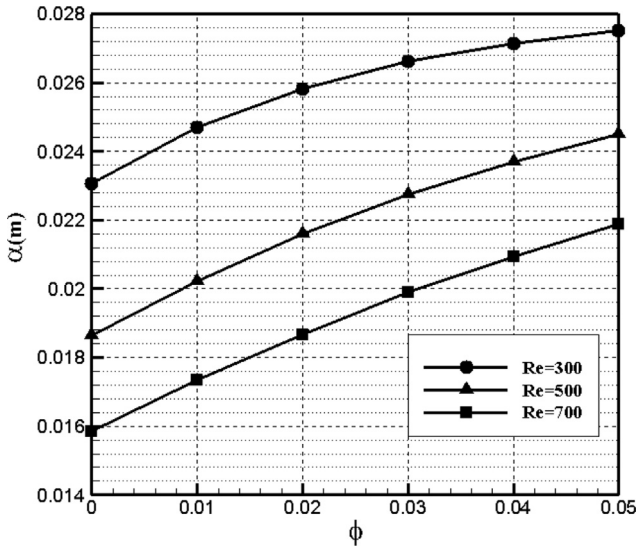

Fig. 12. Detected amplitudes of the wavy wall for minimum average Nusselt number at different volume fractions and Reynolds numbers.

consequently the separation point moves towards the wave's peak, yielding the vortex to fill the wave of the wall. Also, temperature gradient near wavy wall augments when Reynolds number increases, due to the mixing of cold fluid in the middle with hot fluid near the wavy wall, which leads to higher average Nusselt numbers.

Amplitudes of the wavy wall which lead to minimum average Nusselt number for various nanoparticle volume fractions and Reynolds numbers are depicted in Fig. 12. For comparison purposes, streamline and temperature contours of the detected amplitude of the wavy wall ($\alpha = 0.0227$ m), and two other amplitudes for the case of $Re = 500$ and $\phi = 3\%$ are displayed in Fig. 13. As shown, it can be found that increasing the amplitude causes an increment in velocity at the converging section of the wave, which consequently augments pressure gradient, and accordingly, the wake happens earlier and a larger recirculation zone will be created. Temperature gradient is also intensified near the wavy wall, because of disturbance of the flow regime, which leads to more mixing of the cold fluid in the core with the hot fluid near the wavy wall.

7. Conclusions

Two-dimensional incompressible laminar flow of Al_2O_3-water nanofluids in a duct with corrugated wall was numerically analyzed and optimized using two phase model. The effects of nanoparticles volume fraction, amplitude of the wavy wall and Reynolds number on average Nusselt number and thermal-hydraulic performance were investigated. Results showed that increasing Reynolds number and nanoparticles volume fraction leads to a considerably higher heat transfer rate. However, increasing the amplitude causes a decrement in Nusselt number until a critical point and then heat transfer begins to enhance. The critical points of amplitudes were detected for various cases. Considering this effect on Nusselt number, increasing the amplitude from $\alpha = 0$ to $\alpha = 0.04$ m for instance at $Re = 500$ and $\phi = 2\%$, causes 1.5 K increment in outlet bulk temperature and 21.07% increment in total heat flux, which shows the important influence of applying wavy walls on heat transfer point of view.

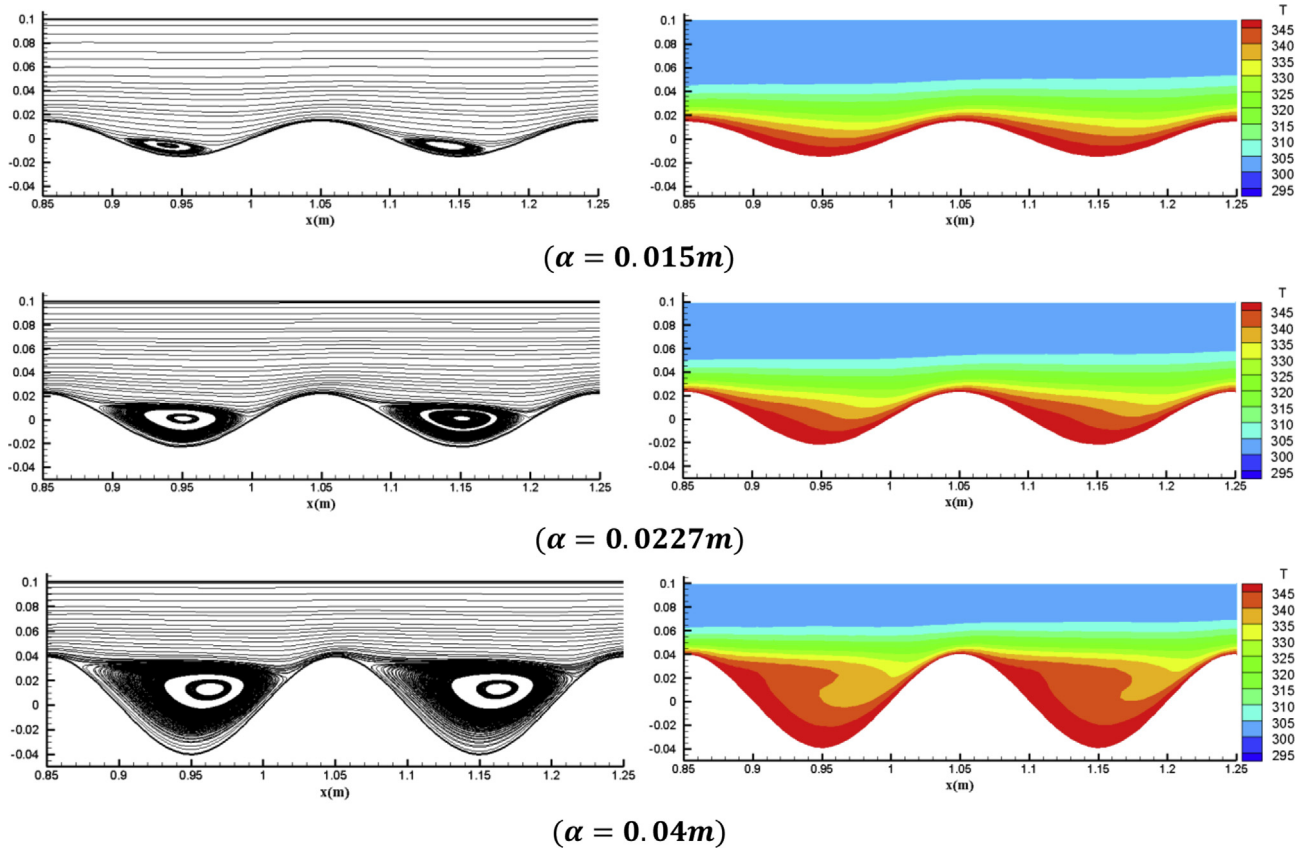

Fig. 13. Comparison of the streamline and temperature contours for different amplitudes of the wavy wall at $Re = 500$ and $\phi = 3\%$.

Additionally, it was observed that nanoparticles have a great influence on enhancing the (j/f) ratio, but increasing wavy channels amplitude has a diverse effect on it due to higher orders of pressure drop than Nusselt number. It was also observed that Reynolds number has an optimum value for thermal-hydraulic performance, calculated by Artificial Bee Colony (ABC) algorithm. The optimal results of ABC were compared with another heuristic optimization method, and results indicated the ABC's efficiency and accuracy for optimizing the considered engineering design problem.

References

[1] C.C. Wang, C.K. Chen, Forced convection in a wavy-wall channel, Int. J. Heat Mass. Transf. 45 (2002) 2587–2595.
[2] N. Mohamed, B. Khedidja, S. Abdelkader, Z. Belkacem, Heat transfer and flow field in the entrance region of a symmetric wavy-channel with constant wall heat flux density, Int. J. Dyn. Fluid 3 (1) (2007) 63–79.
[3] F.V. Castellões, J.N.N. Quaresma, R.M. Cotta, Convective heat transfer enhancement in low Reynolds number flows with wavy walls, Int. J. Heat Mass Transf. 53 (2010) 2022–2034.
[4] H.M. Metwally, R.M. Manglik, Enhanced heat transfer due to curvature-induced lateral vortices in laminar flows in sinusoidal corrugated-plate channels, Int. J. Heat Mass Transf. 47 (2004) 2283–2292.
[5] S.A. Manavi, A. Ramiar, A.A. Ranjbar, Turbulent forced convection of nanofluid in a wavy channel using two phase model, Heat Mass Transf. 50 (2014) 661–671.
[6] H. Heidary, M.J. Kermani, Effect of nano-particles on forced convection in sinusoidal-wall channel, Int. Commun. Heat Mass 37 (2010) 1520–1527.
[7] M.A. Ahmed, N.H. Shuaib, M.Z. Yusoff, Numerical investigations on the heat transfer enhancement in a wavy channel using nanofluid, Int. J. Heat Mass Transf. 55 (2012) 5891–5898.
[8] M. Akbari, N. Galanis, A. Behzadmehr, Comparative analysis of single and two-phase models for CFD studies of nanofluid heat transfer, Int. J. Therm. Sci. 50 (2011) 1343–1354.
[9] X.T. Cheng, X.G. Liang, Optimization principles for two-stream heat exchangers and two-stream heat exchanger networks, Energy 46 (2012) 386–392.
[10] H.J. Feng, L.G. Chen, Z.H. Xie, F. Sun, Constructal entransy dissipation rate minimization for variable cross-section insulation layer of the steel rolling reheating furnace wall, Int. Commun. Heat Mass 52 (2014) 26–32.
[11] Z.Y. Guo, H.Y. Zhu, X.G. Liang, Entransy—a physical quantity describing heat transfer ability, Int. J. Heat Mass Transf. 50 (2007) 2545–2556.
[12] L. Chen, Progress in study on constructal theory and its application, Sci. China: Technol. Sci. 55 (2012) 802–820.
[13] H. Feng, L. Chen, Z. Xie, F. Sun, Constructal entransy optimizations for insulation layer of steel rolling reheating furnace wall with convective and radiative boundary conditions, Chin. Sci. Bull. 59 (2014) 2470–2477.
[14] H. Feng, L. Chen, Z. Xie, Z. Ding, F. Sun, Generalized constructal optimization for solidification heat transfer process of slab continuous casting based on heat loss rate, Energy 66 (2014) 991–998.
[15] H. Feng, L. Chen, Z. Xie, F. Sun, Constructal entransy dissipation rate minimization for triangular heat trees at micro and nanoscales, Int. J. Heat Mass Transf. 84 (2015) 848–855.
[16] H. Feng, L. Chen, Z. Xie, F. Sun, Constructal optimization for a single tubular solid oxide fuel cell, J. Power Sources 286 (2015) 406–413.
[17] G. Fabbri, Heat transfer optimization in corrugated wall channels, Int. J. Heat Mass Transf. 43 (2000) 4299–4310.
[18] Y.T. Yang, Y.H. Wang, P.K. Tseng, Numerical optimization of heat transfer enhancement in a wavy channel using nanofluids, Int. Commun. Heat Mass 51 (2014) 9–17.
[19] D. Karaboga, B. Akay, A comparative study of artificial bee colony algorithm, Appl. Math. Comput. 214 (2009) 108–132.
[20] B. Basturk, D. Karaboga, An artificial bee colony (ABC) algorithm for numeric function optimization, in: IEEE Swarm Intelligence Symposium, Indianapolis, Indiana, USA, 2006.
[21] A.S. Sahin, B. Kılıç, U. Kılıç, Design and economic optimization of shell and tube heat exchangers using artificial bee colony (ABC) algorithm, Energy Convers. Manag. 52 (2011) 3356–3362.
[22] J. Kennedy, R.C. Eberhart, Particle swarm optimization, in: IEEE international conference on neural networks, 1995, pp. 1942–1948.
[23] M. Maninen, V. Taivassalo, On the Mixture Model for Multiphase Flow, VTT Publication, Espo, 1996.
[24] M. Ishii, T. Hibiki, Thermo-fluid Dynamics of Two-phase Flow, Springer Science Business Media, New York, USA, 2006.
[25] B.C. Pak, Y.I. Cho, Hydrodynamic and heat transfer study of dispersed fluids with submicron metallic oxide particles, Exp. Heat Transf. 11 (1998) 151–170.
[26] F.P. Incropera, D.P. Dewitt, Fundamentals of Heat and Mass Transfer, fifth ed., John Wiley & Sons, Inc., 2002.
[27] J.H. Ferziger, M. Peric, Computational Methods for Fluid Dynamics, Springer, New York, USA, 2002, pp. 200–202.
[28] F.O. Tolentino, R.R. Mendez, H.A. Guerrero, B.G. Palomares, Experimental study of fluid in the entrance of a sinusoidal channel, Int. J. Heat Fluid Flow 29 (2008) 1233–1239.